Growth of *N*,*N*′-di(naphthalene-1-yl)-*N*,*N*′-diphenyl-benzidine dome structures

Y. H. Leung, A. B. Djurišić,[a] C. H. Cheung, and M. H. Xie
Department of Physics, The University of Hong Kong, Pokfulam Road, Hong Kong, Hong Kong

W. K. Chan
Department of Chemistry, The University of Hong Kong, Pokfulam Road, Hong Kong, Hong Kong

(Received 24 August 2004; accepted 19 November 2004; published online 6 January 2005)

N,*N*′-di(naphthalene-1-yl)-*N*,*N*′-diphenyl-benzidine samples exhibiting interesting nano/microstructure were fabricated by thermal evaporation in a tube furnace under Ar gas flow. We investigated the influence of the substrate type, substrate temperature, source temperature, and the gas flow rate on the obtained morphology. The deposited material was investigated using scanning electron microscopy, x-ray diffraction, and photoluminescence. We found that the substrate temperature was the factor which significantly affected the obtained morphology, while other factors such as substrate type, source temperature, and gas flow mainly affected the size distribution of the features but not the type of morphology observed. © *2005 American Institute of Physics*.
[DOI: 10.1063/1.1847722]

I. INTRODUCTION

N,*N*′-di(naphthalene-1-yl)-*N*,*N*′-diphenyl-benzidine (NPB) is a commonly used material in organic light emitting diodes (OLEDs), either as a hole transport or blue emitting material.[1–3] A green emitting OLED typically consists of a NPB as a hole transport material and tris (8-hydroxyquinoline) aluminum (Alq) as electron transport and emitting layer. The properties of Alq have been more extensively studied than the properties of NPB, and the syntheses of different Alq nanostructures were reported recently.[4–7] Vapor condensation of Alq resulted in formation of nanoparticles,[4] nanoscaled crystalline film,[5] and nanowires and nanobelts.[6] In vapor condensation synthesis method,[4–6] Alq evaporated from a graphite boat condensed on a Si substrate placed under a liquid nitrogen trap. It was proposed that the nanostructures were formed via collisions with Ar atoms in the carrier gas and rapid cooling at the substrate kept at liquid nitrogen temperature which prevented coalescence. However, Alq nanowire synthesis in argon flow in a tube furnace was also reported,[7] and in this case the substrate temperatures were in the range 60–150 °C. Therefore, low substrate temperature is not essential for preventing the coalescence.

Morphology studies of NPB,[1,8–10] unlike Alq, have been performed mainly on thin films deposited by conventional evaporation. In this work, we investigated the morphology and the optical properties of NPB structures fabricated by evaporation in Ar flow in a tube furnace. The influence of the source and substrate temperatures, gas flow, and substrate type on the obtained morphology was investigated. It was found that, under suitable conditions, films consisted of microdomes with high density. It was shown that efficient OLEDs could be prepared with self-organized microdomes of a hole transport material.[11] *N*,*N*′-Bis(3-toly1)-*N*,*N*′-bis(phenyl) benzidine (TPD) microdomes fabricated by casting from a dilute solution formed regular arrays of microdomes on mica, but the regularity was significantly reduced on indium-tin-oxide (ITO)/poly(2,3-dihydrothieno(3,4-b)-1,4-dioxin): poly(styrenesulfonate) (PEDOT:PSS) electrodes.[11] Here we demonstrate the fabrication of NPB microdomes by evaporation method, in which the size distribution is improved on ITO and PEDOT:PSS substrates compared to glass substrates. The fabricated structures are of interest for application in microdome-based OLEDs.[11] Due to higher glass transition temperature and consequently better OLED operational stability, it is expected that NPB microdomes would yield better performance compared to TPD microdomes.

II. EXPERIMENTAL DETAILS

ITO glass substrates with a nominal sheet resistance of 40 Ω/□ were supplied by Varitronix Limited, Hong Kong. PEDOT:PSS (2.8 wt % dispersed in H_2O) was purchased from Aldrich. Alq was obtained from H. W. Sands and NPB powder was obtained from e-Ray Optoelectronics Technology Co., Ltd. Alq and NPB were purified by vacuum sublimation before use. For NPB dome fabrication, the NPB powder (0.04 g) was placed in a quartz crucible in the quartz tube inside a tube furnace. The furnace was evacuated using a rotary pump and heated to the desired temperature with desired flow (0.25 or 0.5 lpm) of Ar gas. The source temperatures were 280, 290, and 300 °C. The deposited products were collected on microscope slide glass substrates, ITO substrates, or ITO/PEDOT:PSS substrates placed in the temperature range of ~55–130 °C. The fabrication times were between 15 min and 1 h. The structure of the deposited materials was investigated by x-ray diffraction (XRD) using a Philips PW1830 diffractometer and scanning electron microscopy (SEM) using a Cambridge 440 SEM. The size distribution of domes was analyzed using Scion Image Beta

[a]Electronic mail: dalek@hkusua.hku.hk

4.02 software. The photoluminescence (PL) spectrum was measured at room temperature using a HeCd laser (325 nm) as the excitation light source. NPB thin films were prepared by thermal evaporation of sublimed NPB powder at pressure of ~10−6 Torr using an AST PEVA 350T evaporator. The film thickness (100 nm) was monitored by a quartz thickness monitor.

For comparison of OLED performance, devices with NPB domes and NPB films of comparable thickness (~60 nm) were fabricated. We prepared both substrates with and without PEDOT:PSS (30 nm). All the ITO glass substrates were cleaned with toluene, then acetone, ethanol, and de-ionized water, and dried in an oven. After drying, the substrates were exposed to UV ozone, and the PEDOT:PSS spin-coating process followed immediately after the UV ozone cleaning. ITO/PEDOT:PSS substrates were baked at 110 °C in a vacuum oven for 24 h. On both ITO and ITO/PEDOT:PSS substrates, NPB domes were fabricated (substrate temperature range 65–85 °C), while NPB film was evaporated on the other pair of substrates. After evaporation of the NPB films, substrates with NPB domes were transferred into an evaporator and the device fabrication was completed for all four substrates by evaporation 50 nm of Alq, 0.3 nm of LiF, 50 nm of Al, and 50 nm of Ag. For the electroluminescence (EL) measurement, a Keithley 2400 sourcemeter was used to bias the devices, and the EL spectra were recorded using a fiberoptic spectrometer PDA-512-USB (Control Development Inc.).

III. RESULTS AND DISCUSSION

Figure 1 shows the SEM images of the NPB deposited on glass substrates for 300 °C source temperature and different substrate temperatures from ~60 °C (a) to ~120 °C (d). It can be observed that the obtained morphology is strongly dependent on the substrate temperature. At lowest temperatures, we can observe some fractal-like structures, which have some similarity with pentacene structures grown under ultrahigh vacuum conditions whose formation can be described with diffusion-limited aggregation.[12] At higher substrate temperatures, a number of micron-sized domes can be observed, similar to the islands obtained by evaporation of NPB onto a substrate heated above glass transition temperature.[1] The formation of droplet-like islands by deposition on heated substrates was attributed to rapid diffusion and re-organization of the molecules on the substrate and within the islands.[1] Finally, with further increase of the substrate temperature some domes with irregular shapes and rough surface can be observed, as shown in Fig. 1(d). The resulting structure resembles a polycrystalline film, which would be expected since the substrate temperature is above glass transition temperature of NPB. To investigate this, XRD measurements were performed for the NPB at different substrate temperatures.

In order to study the influence of the deposition conditions on the obtained morphology, we have varied the source temperature, deposition time, and gas flow rate. The source temperatures of 280, 290, and 300 °C resulted in very similar morphologies, although the feature sizes were smaller for lower source temperature. Note that lowering the source temperature corresponds to decreasing the flux of the deposit, and thus decreasing material coverage for the same deposition time. Consequently, the feature size becomes larger at

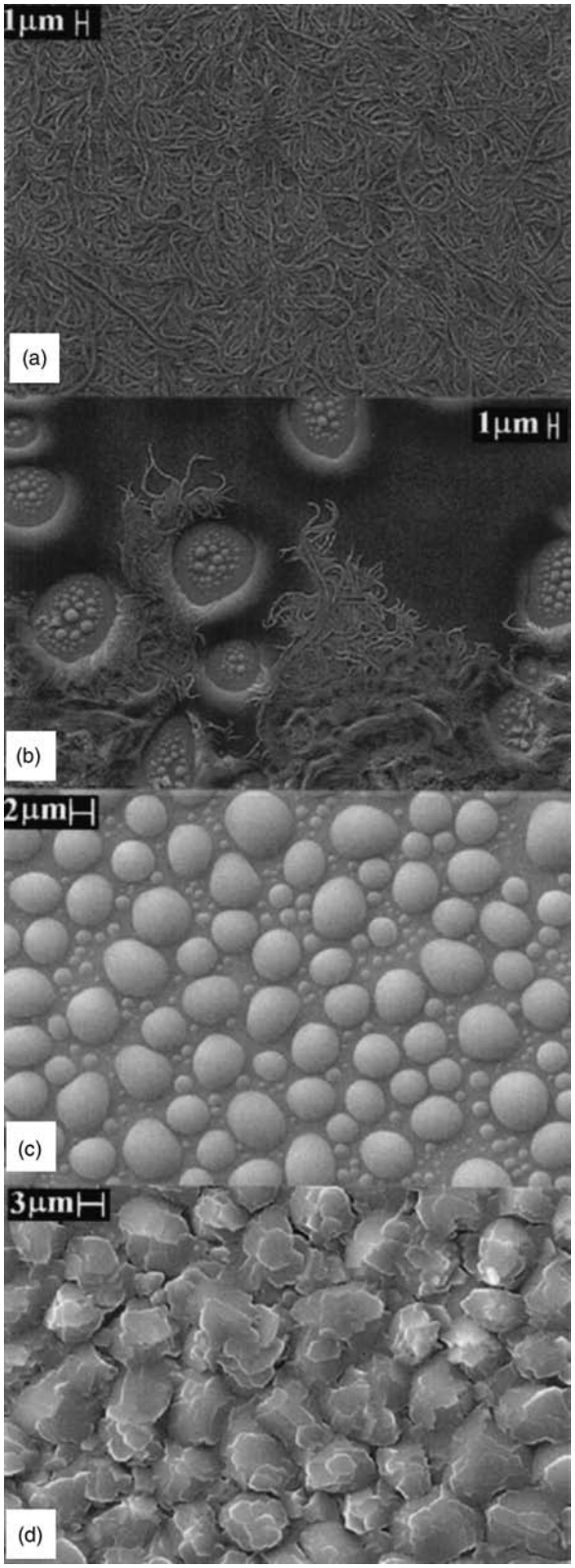

FIG. 1. SEM images of the NPB samples for different substrate temperature regions. The temperature is changing from low (60–70 °C), shown in (a), to high (120 °C), shown in (d). Source temperature was 300 °C, and deposition time was 1 h.

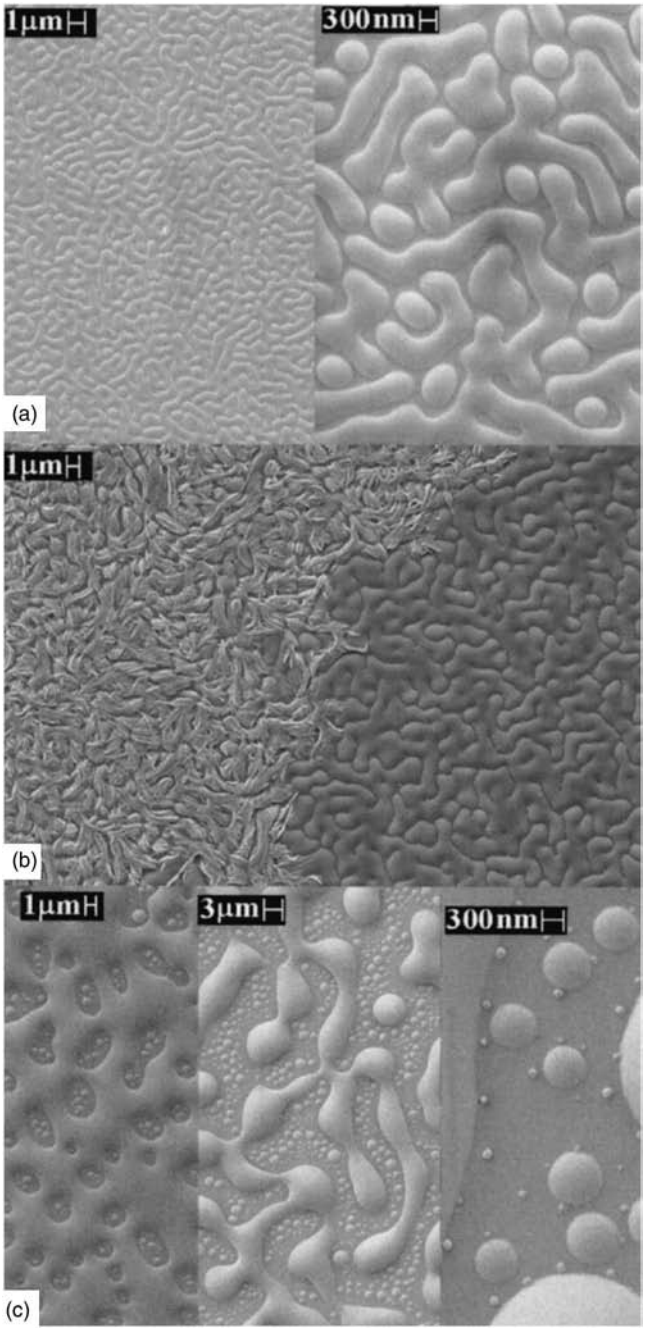

FIG. 2. SEM images of NPB samples deposited on (a) ITO substrate, source temperature 290 °C, gas flow 0.25 lpm, 30 min deposition time, substrate temperature 50–60 °C. (b) Glass substrate, 290 °C source temperature, 60 min deposition time, substrate temperature 65–75 °C. (c) Glass substrate, source temperature 300 °C, gas flow 0.5 lpm, 60 min deposition time, substrate temperature 65–75 °C. Different panels of the image show representative morphologies on the same substrate, with temperature increasing from left to the right.

higher source temperatures. Material coverage can also be changed by varying deposition time. For deposition times of 15 and 30 min, as well as the lowest source temperature of 280 °C, no fractal-like structures were found in the low substrate temperature region. Instead, both samples deposited on glass and ITO substrates exhibited features shown in Fig. 2(a). With increase of the deposition time to 60 min, some dendritic structures are observed on the surface for source temperature of 290 °C, as shown in Fig. 2(b). For 300 °C source temperature, a similar result was obtained. The gas flow rate did not appear to have significant influence on the obtained morphology. Figure 2(c) shows the samples obtained at gas flow of 0.5 lpm. The substrate covers the temperature range of 65–75 °C, corresponding to the transition between isolated regions with domes to high density dome structures. Different panels of the image show representative morphologies on the same substrate, with temperature increasing from left to the right. Similar morphologies are obtained as for the flow rate of 0.25 lpm.

We also investigated the influence of the substrate to the obtained morphologies. It was shown that the choice of substrate significantly affected the morphology of 9,10-anthraquinone structures prepared by thermal evaporation.[13] Different substrates provide different affinity to the deposit. Also, the relative surface/interface energies are different. Previous experiments have already indicated that modification of the ITO with self-assembled molecules affected the morphology of the NPB films. Also, NPB morphology was changed by the deposition of thin layer of copper phthalocyanine.[10] Thus, it is expected that the substrate may have an effect on the obtained morphology. Figures 3(a)–3(c) shows the comparison between the dome morphologies obtained for glass, ITO, and ITO/PEDOT:PSS substrates, while Fig. 3(d) shows the comparison of the dome sizes for different substrates. The morphologies in the higher temperature regions are similar in all cases, while the lower temperature region [see Fig. 2(a)] is similar for ITO and glass substrates. For glass substrates, we can observe larger average dome size and larger dispersion in obtained dome sizes. The size dispersion increases with time, as shown in Fig. 3(a). The left panel shows obtained structures after 15 min of deposition, while the right panel shows obtained structures after 60 min of deposition. The dome size distribution of samples deposited on a glass substrate shown in Fig. 3(d) corresponds to the left panel of Fig. 3(a). On ITO substrates, we can observe improved uniformity in the dome sizes compared to the glass substrate, and the average dome size is smaller. The deposition time does not significantly affect size dispersion, but the size of the domes increases with deposition time. Therefore, on ITO substrates we mainly observed lateral growth of the domes with time, while on glass substrates there was nucleation of new domes in addition to the lateral growth of existing ones. On ITO/PEDOT:PSS substrates, the dome size is further reduced and size dispersion improved compared to ITO substrates, but the domes have more irregular shapes, as shown in Fig. 3(c). The size of the nonspherical domes increases with increasing substrate temperature, and the films become disordered at the highest temperatures. No other morphologies apart from the domes and disordered films were found on PEDOT:PSS.

We also performed XRD measurements on the structures deposited at different temperatures. The glass transition temperature of NPB is 96 °C, while crystallization temperature is 184 °C.[14] Obtained XRD result is shown in Fig. 4(a). XRD spectra of NPB films and NPB powder are also shown for comparison. It can be observed that the film and the samples deposited at different temperatures are dominantly amorphous. The broad feature in the range 15–35° is due to

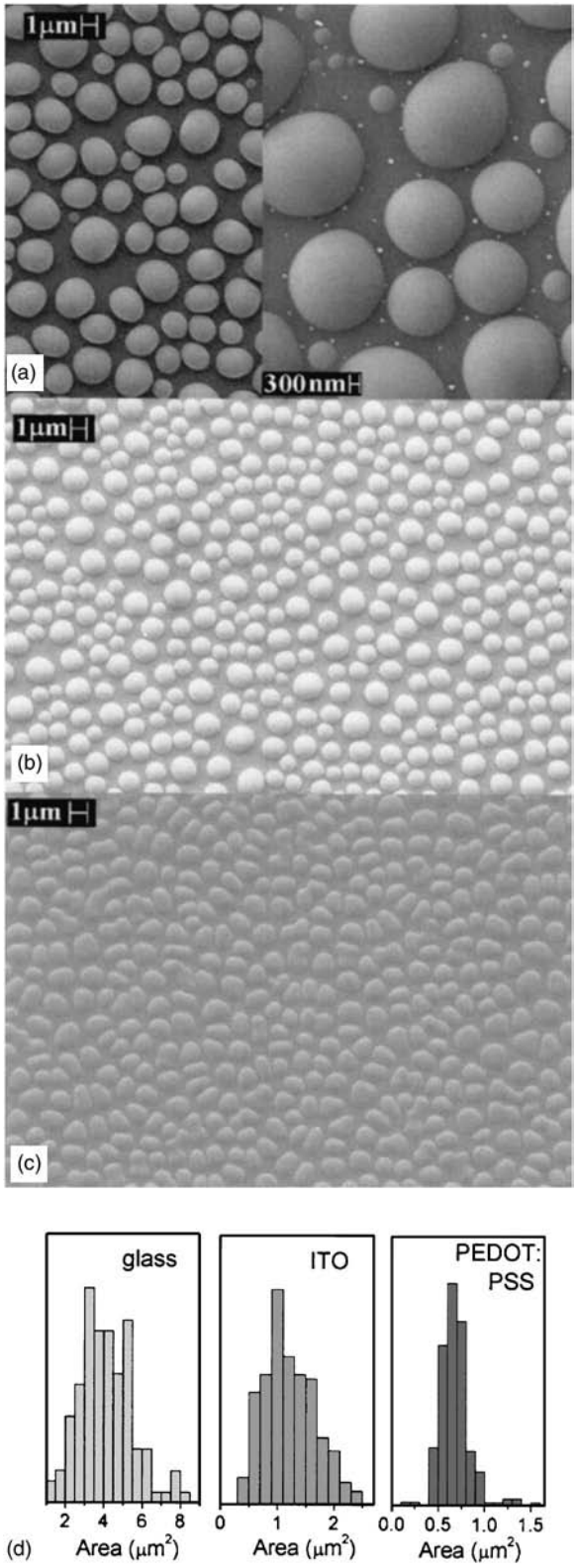

FIG. 3. SEM images of NPB samples deposited at source temperature 290 °C on (a) glass substrate, 15 min deposition time on the left, 60 min deposition time on the right. (b) ITO substrate, 30 min deposition time. (c) ITO/PEDOT:PSS substrate, 30 min deposition time. Substrate temperature was in the range 80–105 °C. (d) Size distribution of domes on different substrates.

the glass substrate.[15] Some low intensity peaks can be observed in a sample deposited at 70–75 and 100–105 °C. Since the XRD measurements were performed on samples

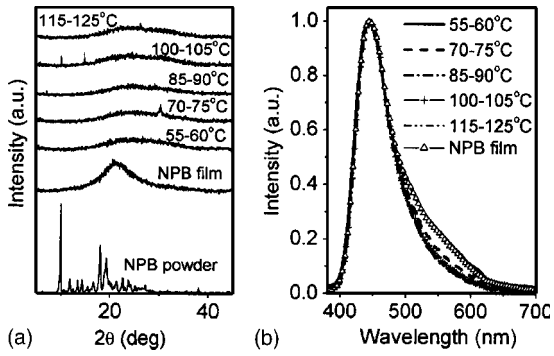

FIG. 4. (a) XRD spectra of NPB samples at different temperatures, NPB film, and NPB powder. (b) Room temperature photoluminescence of NPB samples at different substrate temperatures. The PL of an NPB film is also shown for comparison.

exposed to atmosphere, it is possible that atmosphere exposure induced formation of small crystalline domains, which is similar to humidity induced crystallization observed in Alq.[16] No peaks are observed for other samples, including the sample deposited in the highest temperature range (~115–125 °C). Therefore, the dome structures likely consist of amorphous NPB. Formation of amorphous spheres was reported for inorganic CdS nanoparticles,[17] as well as organic Alq nanoparticles.[4] The spherical shape was attributed to the thermodynamic driving force for surface energy minimization.[17] Formation of NPB droplet-like structures on substrates above glass transition temperature was attributed to rapid diffusion and surface energy minimization.[1] However, it should be noted that even for substrate temperature considerably lower than the glass transition temperature (i.e., 60–80 °C), films showing different island structures are obtained. These morphologies are notably different from NPB films evaporated under high vacuum on unheated substrates which typically show relatively flat surfaces with rms roughness below 7 nm.[8,9]

Figure 4(b) shows the PL spectra for the samples deposited at different substrate temperature. The PL of NPB film is also shown for comparison. The obtained emission peak (~444 nm) is within the range of reported peak wavelengths for NPB in the literature which range from 430 to 450 nm.[8] The peak position is the same for all the samples, but the low energy tail is reduced for higher substrate temperature. It was shown that the PL spectra of Alq show small dependence on the substrate temperature.[18] The obtained changes in the PL of NPB are more likely due to different substrate temperature rather than difference in morphology of the different samples.

Figure 5 shows the current–voltage and luminance–voltage characteristics of OLEDs with NPB domes and conventional NPB films. It can be observed that for both ITO and ITO/PEDOT:PSS substrates, the turn-on voltage (defined as voltage needed to achieve luminance of 1 cd/m^2) is reduced. The performance of the devices on ITO/PEDOT:PSS substrates is significantly better than that of devices on bare ITO. The turn-on voltage for OLEDs with NPB domes on PEDOT:PSS substrates is 3.5 V, while for OLEDs with NPB film it is 7 V. Low turn-on voltage for OLEDs with NPB domes is in agreement with previously reported result for

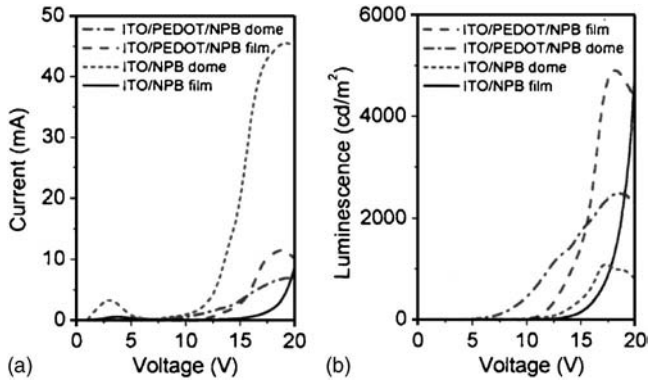

FIG. 5. (a) Current–voltage and (b) luminance–voltage characteristics of OLEDs with NPB films and NPB domes.

OLEDs with TPD domes.[11] The maximum luminance of the devices with domes is lower than that of the devices with NPB films. However, maximum efficiency is increased and it is achieved at lower voltages (2.5 cd/A at 9 V for NPB dome device, 1.8 cd/A at 12 V for NPB film device). A possible reason for reduced maximum luminance could be due to reduced effective light emitting area, since it was shown that emission in OLEDs with TPD domes mainly originates from the domes with small residual emission between the domes.[11]

IV. CONCLUSION

We investigated the influence of the fabrication conditions to the morphology of NPB structures deposited in a tube furnace. We found that the substrate type and the substrate temperature significantly affect the morphology. Under suitably chosen conditions, high density of microdomes with good size distribution can be obtained. These microdome structures are of interest for potential applications in OLEDs. OLEDs with NPB domes on PEDOT:PSS substrates show lower turn-on voltage and higher efficiency compared to OLEDs with conventional NPB films. Lowering of the turn-on voltage is in agreement with previously reported results on TPD microdomes fabricated by a different method.

ACKNOWLEDGMENTS

The authors would like to thank Amy Wong and Wing Song Lee for SEM measurements, and the staff of Materials Preparation and Characterization Centre, Hong Kong University of Science and Technology for XRD measurements. This work is partly supported by The Research Grants Council of the Hong Kong Special Administrative Region, China (Project No. HKU 7056/02E).

[1] M. Carrard, S. Gonclaves-Conto, L. Si-Ahmed, D. Adès, and A. Siove, Thin Solid Films **352**, 189 (1999).
[2] Y. Kijima, N. Asai and S-I. Tamura, Jpn. J. Appl. Phys., Part 1 **38**, 5274 (1999).
[3] T. Tsuji, S. Naka, H. Okada, and H. Onnagawa, Appl. Phys. Lett. **81**, 3329 (2002).
[4] J.-J. Chiu, W. S. Wang, C.-C. Kei, and T.-P. Perng, Appl. Phys. Lett. **83**, 347 (2003).
[5] J.-J. Chiu, W. S. Wang, C.-C. Kei, C.-P. Cho, T. P. Perng, P.-K. Wei, and S.-Y. Chiu, Appl. Phys. Lett. **83**, 4607 (2003).
[6] J.-J. Chiu, C.-C. Kei, W. S. Wang, and T.-P. Perng, Adv. Mater. (Weinheim, Ger.) **15**, 1361 (2003).
[7] C. H. Cheung, A. B. Djurišić, Y. H. Leung, Z. F. Wei, S. J. Xu, and W. K. Chan, Chem. Phys. Lett. **394**, 203 (2004).
[8] M. S. Chun, T. Teraji, and T. Ito, Jpn. J. Appl. Phys., Part 1 **42**, 5233 (2003).
[9] Q.-T. Le, E. W. Forsythe, F. Nüesch, L. J. Rothberg, L. Yan, and Y. Gao, Thin Solid Films **363**, 42 (2000).
[10] E. W. Forsythe, M. A. Abkowitz, Y. Gao, and C. W. Tang, J. Vac. Sci. Technol. A **18**, 1869 (2000).
[11] O. Karthaus, C. Adachi, S. Kurimura, and T. Oyamada, Appl. Phys. Lett. **84**, 4696 (2004).
[12] F.-J. Meyur zu Heringdorf, N. C. Reuter, and R. M. Tromp, Nature (London) **412**, 517 (2001).
[13] H. Liu, Y. Li, S. Xiao, H. Li, L. Jiang, D. Zhu, B. Xiang, Y. Chen, and D. Yu, J. Phys. Chem. B **108**, 7744 (2004).
[14] Y. Sato, S. Ichinosawa, and H. Kanai, IEEE J. Sel. Top. Quantum Electron. **4**, 40 (1998).
[15] M. Gunasekaran, R. Gopalakrishnan, and P. Ramasamy, Mater. Lett. **58**, 67 (2003).
[16] H. Aziz, Z. Popovic, S. Xie, A.-M. Hor, N.-X. Hu, C. Tripp, and G. Xu, Appl. Phys. Lett. **72**, 756 (1998).
[17] C. Ye, G. Meng, Y. Wang, Z. Jiang, and L. Zhang, J. Phys. Chem. B **106**, 10338 (2003).
[18] A. B. Djurišić, T. W. Lau, L. S. M. Lam, and W. K. Chan, Appl. Phys. A: Mater. Sci. Process. **78**, 375 (2004).